Histol Histopathol (2018) 33: 555-565

http://www.hh.um.es

Histology and Histopathology

From Cell Biology to Tissue Engineering

Cotton rats (*Sigmodon hispidus*) possess pharyngeal pouch remnants originating from different primordia

Teppei Nakamura[1,2], Osamu Ichii[2], Takao Irie[3], Tatsuya Mizoguchi[2], Akio Shinohara[4], Hirokazu Kouguchi[3], Yuji Sunden[5], Saori Otsuka-Kanazawa[2], Yaser Hosny Ali Elewa[2,6], Chihiro Koshimoto[4], Ken-ichi Nagasaki[1] and Yasuhiro Kon[2]

[1]Section of Biological Safety Research, Chitose Laboratory, Japan Food Research Laboratories, Chitose, [2]Laboratory of Anatomy, Department of Basic Veterinary Sciences, Faculty of Veterinary Medicine, Hokkaido University, [3]Medical Zoology Group, Department of Infectious Diseases, Hokkaido Institute of Public Health, Sapporo, Hokkaido, [4]Division of Bio-Resources, Department of Biotechnology, Frontier Science Research Center, University of Miyazaki, Kiyotake, Miyazaki, [5]Laboratory of Veterinary Pathology, Faculty of Agriculture, Tottori University, Tottori, Japan and [6]Department of Histology and Cytology, Faculty of Veterinary Medicine, Zagazig University, Zagazig, Egypt

Summary. Pharyngeal pouches in mammals develop into specific derivatives. If the differentiation of the pharyngeal pouches is anomalous, their remnants can result in cysts, sinuses, and fistulae in the differentiated organs or around the neck. In the present study, we found several pharyngeal pouch remnants, such as cystic structures in thymus and parathyroid gland and fossulae extended from the piriform fossa, in the inbred cotton rats maintained at Hokkaido Institute of Public Health (HIS/Hiph) and University of Miyazaki (HIS/Mz). In HIS/Hiph, the fossulae extended from the apex of the piriform fossa into the thyroid glands and were lined with stratified squamous and cuboidal epithelium. Calcitonin-positive C-cells were present within their epithelium in HIS/Hiph. In contrast, the fossulae of HIS/Mz ran outside the thyroid glands toward the parathyroid glands; they were lined with columnar ciliated epithelium and a few goblet cells, but had no C-cells, which was consistent with the cystic structures in the thymus and the parathyroid gland. These results indicated that the fossulae were a remnant of the ultimobranchial body in HIS/Hiph and of the thymopharyngeal duct in HIS/Mz. Thus, the fossulae of the piriform fossa resembled the piriform sinus fistula in human. In conclusion, cotton rats frequently possessed pharyngeal pouch remnants, including the piriform sinus fistula, and therefore, might serve as a novel model to elucidate the mechanisms of pharyngeal pouch development.

Key words: Cotton rat, Pharyngeal pouch remnant, Thymopharyngeal duct, Ultimobranchial body, Piriform sinus fistula

Offprint requests to: Yasuhiro Kon, D.V.M., Ph.D, Laboratory of Anatomy, Department of Basic Veterinary Sciences, Faculty of Veterinary Medicine, Hokkaido University, Kita 18-Nishi 9, Kita-ku, 060-0818 Sapporo, Japan. e-mail: y-kon@vetmed.hokudai.ac.jp

DOI: 10.14670/HH-11-946

Introduction

During mammalian fetal development, pharyngeal pouches, particularly the first to fourth ones, develop into specific derivatives, including the pharyngo-tympanic tube, middle ear cavity, palatine tonsil, thymus, parathyroid glands, and ultimobranchial bodies. In humans, the third pharyngeal pouch forms parathyroid gland III (also known as inferior parathyroid gland) and thymus (Nicoucar et al., 2010). During fetal development, the thymus migrates caudally, connecting to the pharynx via the thymopharyngeal duct. The parathyroid gland III is attached to the thymus on its cranial pole (Grevellec and Tucker, 2010). The fourth pharyngeal pouch gives rise to parathyroid gland IV (superior parathyroid gland), and thymus (Nicoucar et al., 2009). The fifth pouch forms the ultimobranchial body, which migrates to the developing thyroid gland and finally differentiates into calcitonin-producing C-

cells (Nicoucar et al. 2009). The differentiation of pharyngeal pouches shows several species-specific differences; for instance, the parathyroid glands develop only from the third pharyngeal pouch and are located within the thyroid gland in some rodents such as mice, rats, and hamsters (Grevellec and Tucker, 2010). Furthermore, the thymus is not derived from the fourth pouch in some mammals, whereas the ultimobranchial body develops from the fourth pharyngeal pouch in mice and from the sixth pouch in aves (Grevellec and Tucker, 2010). In some other mammals, a small population of C-cells is found in parathyroid gland IV, in addition to the ultimobranchial body (Kameda, 1971).

Abnormal differentiation of the pharyngeal pouches can result in several remnant tissues, which might eventually develop into cysts, sinuses, or fistulae, depending on the degree of developmental malformation. In particular, developmental anomalies in the third and fourth pharyngeal pouches result in cysts known as thymopharyngeal duct cyst in thymus, parathyroid cyst in parathyroid glands, and ultimobranchial body cyst (also known as solid cell nest) in the thyroid (Capen and Rosol, 1989; Pearse, 2006; Vázquez-Román et al., 2013). In humans, remnants from anomalous development of the third and fourth pharyngeal pouches can remain in the neck region, and form sinuses and fistulae extending from piriform fossa (Nicoucar et al., 2009, 2010). These abnormalities during the differentiation of pharyngeal pouches might cause recurrent neck abscess, suppurative thyroiditis, stridor, or dysphagia (Shrime et al., 2003; Rea et al., 2004); however, the pathogenesis of such anomalies remains unclear because of the lack of suitable animal models.

Rodents, especially mice, serve as good model systems for developmental studies, but there have been no reports about severe spontaneous pharyngeal pouch remnants such as sinuses and fistulae in rodent models. In this study, we found for the first time, several pharyngeal pouch remnants in the hispid cotton rat (*Sigmodon hispidus*), by morphological observation. The cotton rat is popular for its use as a model for infectious diseases, owing to its susceptibility to a wide range of human pathogens including viruses, bacteria, fungi, and parasites (Niewiesk and Prince, 2002). Their susceptibility toward the human adenovirus has made them a valuable research tool for adenovirus-based gene therapy (Setoguchi et al., 1994). In addition, cotton rats are known to spontaneously develop cardiomyopathy, characterized by degeneration and inflammation, and similar lesions are observed in skeletal muscles (Faith et al., 1997). Furthermore, inbred cotton rats develop female-dominant enterochromaffin-like cell-derived carcinomas, as well as anemia with renal inflammation and chronic kidney disease (Ichii et al., 2016; Waldum et al., 1999). Therefore, in addition to their existing role in pathology research, we introduce the potential of cotton rats as a valuable animal model for studying development of pharyngeal pouch-derived organs.

Materials and methods

Animals

Animal experimentation was performed in accordance with guidelines issued by Hokkaido Institute of Public Health (approval no. K27-03) and University of Miyazaki (approval no. 2014-503). Inbred cotton rats (*Sigmodon hispidus*), maintained at Hokkaido Institute of Public Health (HIS/Hiph) and University of Miyazaki (HIS/Mz), were used in the present study. The male and female animals were used at the age from postnatal day 1 to 25 months in HIS/Hiph, and from 1 to 3 months in HIS/Mz. To examine the age-related changes, the HIS/Hiph strains were divided into three life stages: juvenile (approximately 0-2 months of age), young adult (approximately 3-6 months of age), and old adults (more than 7 months of age) (Faith et al., 1997).

Light microscopy

The laryngeal pharynx and the thymus were fixed with 10% neutral buffered formalin and embedded in paraffin. In the laryngeal pharynx, 4-μm-thick horizontal sections were cut at every 50 μm. For the thymus, transverse sections were prepared. The sections were stained with hematoxylin and eosin (HE) and periodic acid-Schiff (PAS). Age-related changes were analyzed using the chi-square test ($P<0.05$).

Immunostaining

Immunostaining was performed to detect parathyroid hormone (PTH, in principal cells of the parathyroid gland), calcitonin (in parafollicular cells/C-cells), thyroglobulin (in thyroid follicle), α-smooth muscle actin (α-SMA, in smooth muscles), and proliferating cell nuclear antigen (PCNA, in proliferating cells). In addition, the p63 protein, which is expressed in basal cells of the endodermal epithelium lining the pharyngeal cavity, and is recognized as a marker for pharyngeal pouch remnants, was detected (Kameda et al., 2009; Ríos Moreno et al., 2011). The details of the primary antibodies are listed in Table 1. For immunohistochemistry, the deparaffinized sections were heated with 10 mM citrate buffer (pH 6.0) for 30 min at 90°C, treated with 0.3% hydrogen peroxidase/methanol solution for 30 min to eliminate endogenous peroxidase, blocked with blocking reagent (Nichirei, Tokyo, Japan), and incubated overnight with primary antibodies at 4°C. Next, the sections were treated with appropriate secondary antibodies (Nichirei) for 30 min, followed by treatment with streptavidin-peroxidase (Nichirei) for 30 min at room temperature. The immunopositive reactions were developed using a 3,3'-diaminobenzidine-H_2O_2 solution. The sections were then counterstained with hematoxylin. For immunofluorescence, the deparaffinized sections were treated with 10 mM citrate buffer (pH 6.0) for 30 min at 90°C, treated with 5%

normal donkey serum, and incubated overnight with primary antibodies at 4°C. The sections were then incubated with a combination of Alexa Fluor 488-labeled donkey anti-goat IgG, Alexa Fluor 594-labeled donkey anti-mouse IgG (1:1,000; Life Technologies, Carlsbad, USA), and Hoechst33342 (1:1,000; Dojindo, Kumamoto, Japan) for 30 min. The fluorescent signals were detected using a confocal microscope (Zeiss, Oberkochen, Germany).

Scanning electron microscopy

The formalin-fixed laryngeal pharynx was post-fixed with glutaraldehyde for 4 h at 4°C followed by 1% osmium tetroxide in 0.1 M PB for 1 h, and treated with 1% tannic acid. The specimens were dehydrated using graded alcohol and freeze-dried by ES-2030 freeze dryer (Hitachi, Tokyo, Japan). The dried specimens were sputter-coated with an E-1030 ion sputter coater (Hitachi, Tokyo, Japan), and examined on an S-4100 SEM (Hitachi) with an accelerating voltage of 10 kV.

Results

Morphological features of pharyngeal pouch-derived organs in cotton rats

The cotton rats showed several morphological features in the laryngeal pharynx and pharyngeal pouch-derived organs that were either similar or different compared with other rodents. As seen in mice, rats, and hamsters, the cotton rats had two lobes of thyroid glands and one pair of parathyroid glands (Fig. 1a). While parathyroid glands are found within the thyroid glands in mice, rats, and hamsters (Grevellec and Tucker, 2010), those containing PTH-positive cells were located apart from the thyroid glands in all cotton rats (Fig. 1a,b). Further, thymic tissues appeared around the laryngeal pharynx in addition to the thoracic cavity in approximately 40% of HIS/Hiph and in all animals of HIS/Mz (Fig. 1a, Table 2), whereas they are recognized as ectopic in other rodents (Pearse, 2006). There were no sex-related differences in the appearance of the cervical thymic tissues (Table 2).

Interestingly, the fossula appeared near the apex of the piriform fossa in all HIS/Hiph animals and in 5 out of 12 animals of HIS/Mz (Fig. 1c, Table 2). In HIS/Hiph, these fossulae localized at the left side in half the males and were primarily bilateral in the females (Table 3). In contrast, the fossulae appeared at the left side in all the five specimens of HIS/Mz (Table 3). Furthermore, cystic structures were observed in the intrathoracic thymus (Fig. 1d-f) and parathyroid glands (Fig. 1g-i) in animals from both strains. The cystic structures in the parathyroid glands mainly localized at the caudal end (Fig. 1g). Although the occurrence rate of the cystic structures at the intrathoracic thymus was not determined, that of the parathyroid glands was approximately 50% in both the strains (Table 2). The lining of these cystic structures was composed of columnar ciliated epithelial cells and goblet cells (Fig. 1e and h), and the basal cells of the epithelium expressed p63, a marker for pharyngeal pouch remnants (Fig. 1f,i). In the thyroid glands cystic structures were also observed in all the animals of both strains (Fig. 1g, Table 2). There was neither a strain- nor a sex-related

Table 1. List of antibodies used for immunohistochemistry and immunofluorescence.

Antibody	Source	Dilution	Application
Rat anti-parathyroid hormone	DAKO (Glostrup, Denmark)	1:50	IHC
Mouse anti-p63	Nichirei (Tokyo, Japan)	Prediluted	IHC and IF
Goat anti-proliferating cell nuclear antigen	Santa Cruz Biochemistry (Santa Cruz, USA)	1:2,000	IF
Rabbit anti-calcitonin	DAKO (Glostrup, Denmark)	Prediluted	IHC and IF
Rabbit anti-thyroglobulin	DAKO (Glostrup, Denmark)	Prediluted	IHC
Rabbit anti-α-smooth muscle actin	Abcam (Cambridge, UK)	1:2,000	IHC

Table 2. Incidence of histopathological findings around laryngeal pharynx.

	HIS/Hiph			HIS/Mz		
	Total	Male	Female	Total	Male	Female
Thymic tissue in cervix	9/24 (37.5%)	5/12 (41.7%)	4/12 (33.3%)	12/12 (100%)	6/6 (100%)	6/6 (100%)
Fossula from piriform fossa	36/36 (100%)	18/18 (100%)	18/18 (100%)	5/12 (41.7%)	3/6 (50%)	2/6 (33.3%)
Cystic structures in parathyroid glands	12/23 (52.1%)	6/12 (50.0%)	6/11 (54.5%)	5/12 (41.7%)	2/6 (33.3%)	3/6 (50%)
Cystic structures in thyroid glands	36/36 (100%)	18/18 (100%)	18/18 (100%)	12/12 (100%)	6/6 (100%)	6/6 (100%)

The incidence of the thymic tissue in cervix was observed in the juvenile and young adult animals owing to the age-related involution of the thymus (Pearse, 2006).

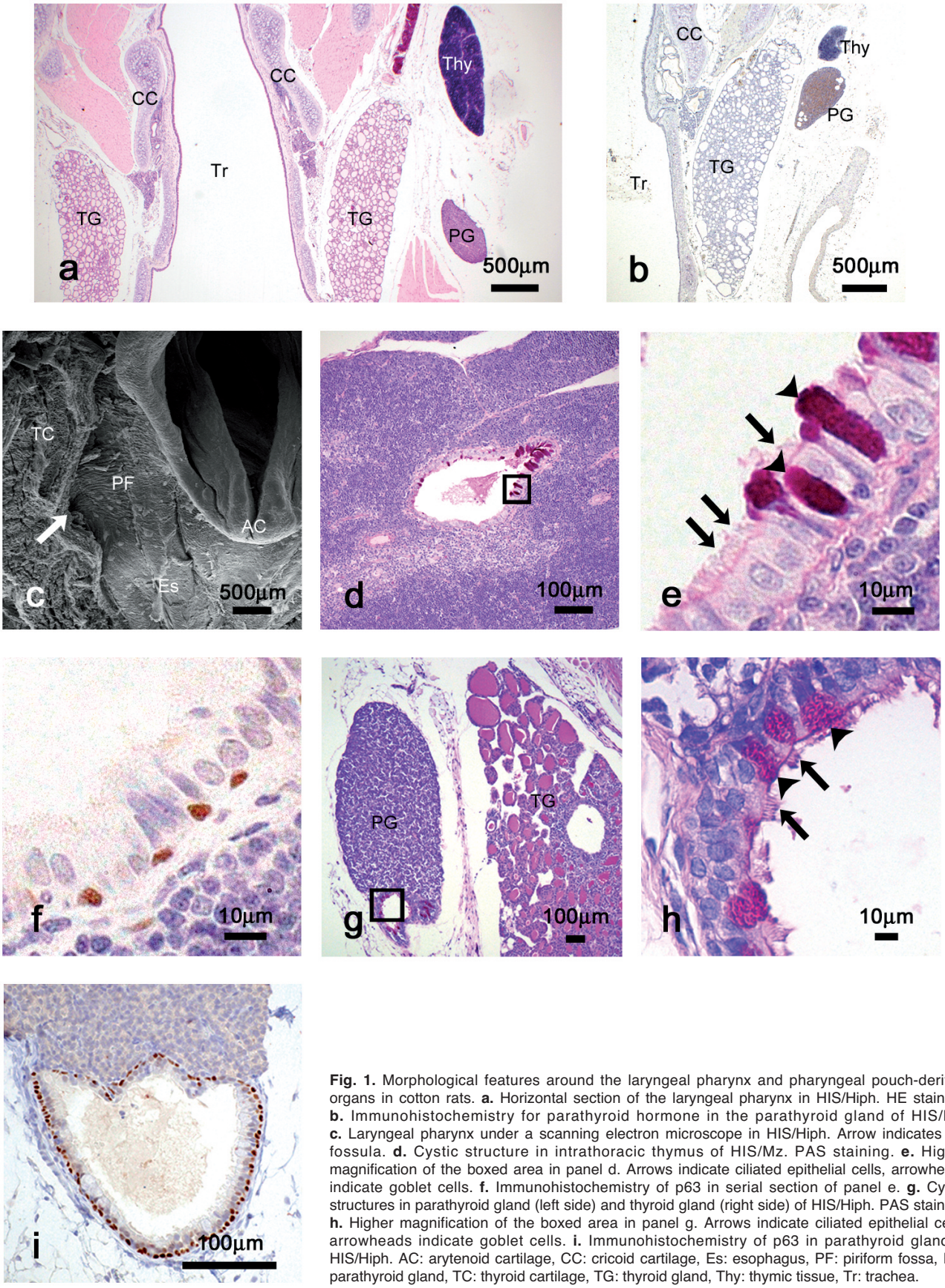

Fig. 1. Morphological features around the laryngeal pharynx and pharyngeal pouch-derived organs in cotton rats. **a.** Horizontal section of the laryngeal pharynx in HIS/Hiph. HE staining. **b.** Immunohistochemistry for parathyroid hormone in the parathyroid gland of HIS/Mz. **c.** Laryngeal pharynx under a scanning electron microscope in HIS/Hiph. Arrow indicates the fossula. **d.** Cystic structure in intrathoracic thymus of HIS/Mz. PAS staining. **e.** Higher magnification of the boxed area in panel d. Arrows indicate ciliated epithelial cells, arrowheads indicate goblet cells. **f.** Immunohistochemistry of p63 in serial section of panel e. **g.** Cystic structures in parathyroid gland (left side) and thyroid gland (right side) of HIS/Hiph. PAS staining. **h.** Higher magnification of the boxed area in panel g. Arrows indicate ciliated epithelial cells, arrowheads indicate goblet cells. **i.** Immunohistochemistry of p63 in parathyroid gland of HIS/Hiph. AC: arytenoid cartilage, CC: cricoid cartilage, Es: esophagus, PF: piriform fossa, PG: parathyroid gland, TC: thyroid cartilage, TG: thyroid gland, Thy: thymic tissue, Tr: trachea.

difference in the appearance of the cystic structures in both the parathyroid glands and the thyroid glands (Table 2).

Ductal structures connecting piriform fossa and thyroid glands in HIS/Hiph cotton rats

We observed the horizontal sections from the laryngeal pharynx to the thyroid glands, and found that the fossulae at the piriform fossa and the cystic structures of the thyroid glands were connected by a duct-like structure in HIS/Hiph (Fig. 2a). Briefly, these ductal structures passed the medial side of the thyroid glands and reached the internal side of the upper pole of the thyroid glands, running along the superior thyroid artery (Fig. 2a,b). The lining of the ductal structures was composed of stratified squamous and cuboidal epithelial cells, and their basal cells expressed p63 (Fig. 2b,c). In the thyroid glands, the ductal structures ended with various features such as dilations or branches (Fig. 2d-f). We thus examined the relationship between aging and the various structures of the ductal end. The results of a chi-square test indicated that the occurrence rate of the branched end of the ductal structures increased

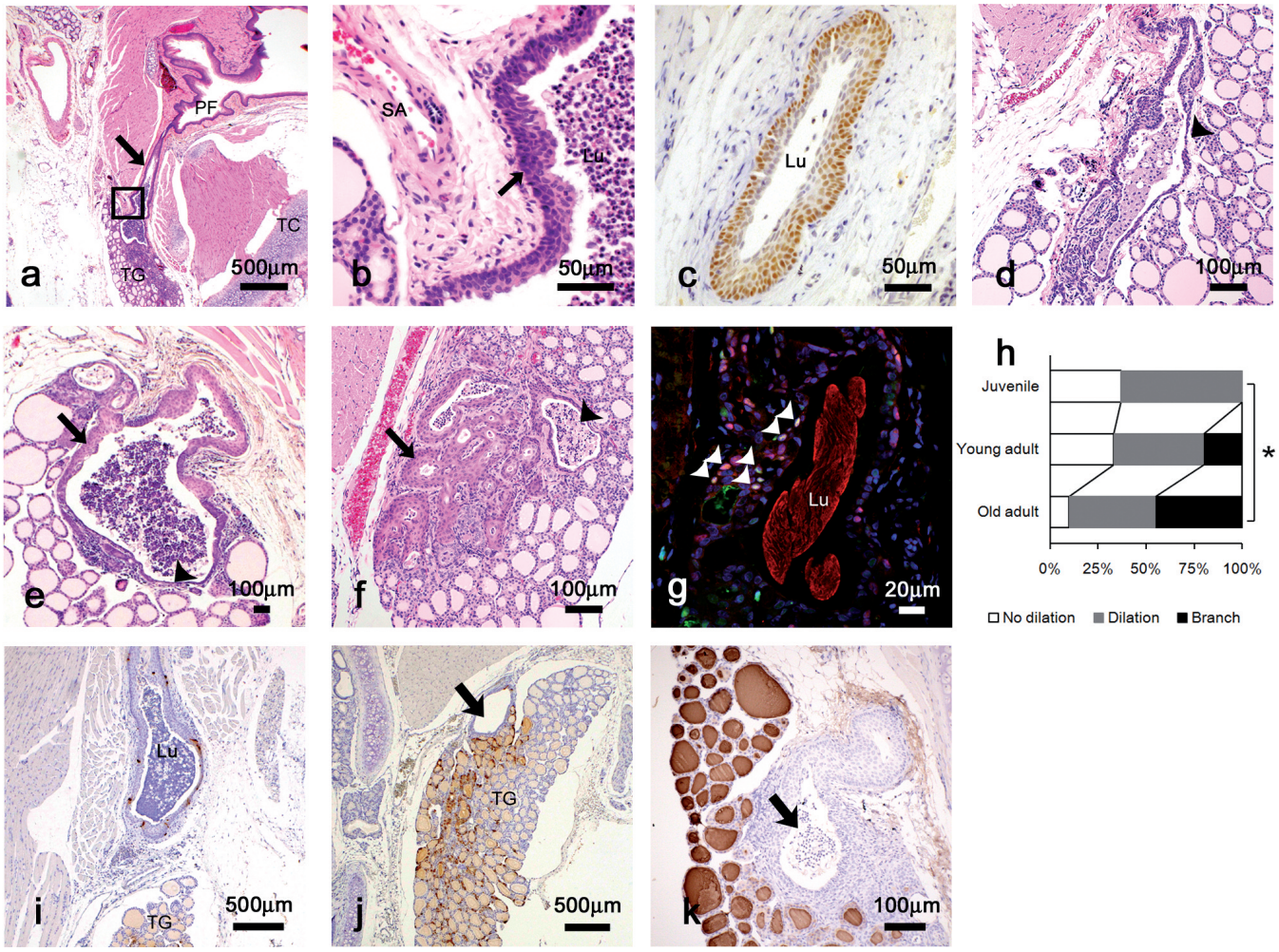

Fig. 2. Ductal structures extending from piriform fossa in HIS/Hiph cotton rats. **a.** Horizontal section of the laryngeal pharynx. Arrow indicates the ductal structures extending from piriform fossa. HE staining. **b.** Higher magnification of boxed area in panel a. **c.** Immunohistochemistry of p63 in the ductal structures. **d-f.** Terminal structure of the ductal structures in the thyroid glands without dilation **(d),** with dilation **(e)**, and with branches **(f)**. Arrows and arrowheads indicate stratified epithelium and simple epithelium, respectively. **g.** Immunofluorescence of p63 (red) and proliferating cell nuclear antigen (green) at the end of the ductal structure. Arrowheads indicate proliferating epithelial cells. **h.** Age-related changes of the terminal structures of the ductal structures. *$P < 0.05$, analyzed using the chi-square test. **i.** Immunohistochemistry of calcitonin in the ductal structures. **j.** Immunohistochemistry of calcitonin in thyroid gland. Arrow indicates the terminal end of the ductal structure. **k.** Immunohistochemistry of thyroglobulin in thyroid gland. Arrow indicates the terminal end of the ductal structure. Lu: lumen of the ductal structure, PF: piriform fossa, SA: superior thyroid artery, TC: thyroid cartilage, TG: thyroid gland.

significantly with age (Fig. 2h). The terminal end of the ductal structures was lined with stratified squamous epithelium or single cuboidal epithelium without columnar ciliated epithelium or goblet cells (Fig. 2d-f). At the branched end, p63-positive cells were arranged unevenly, some of which were positive for PCNA (Fig.

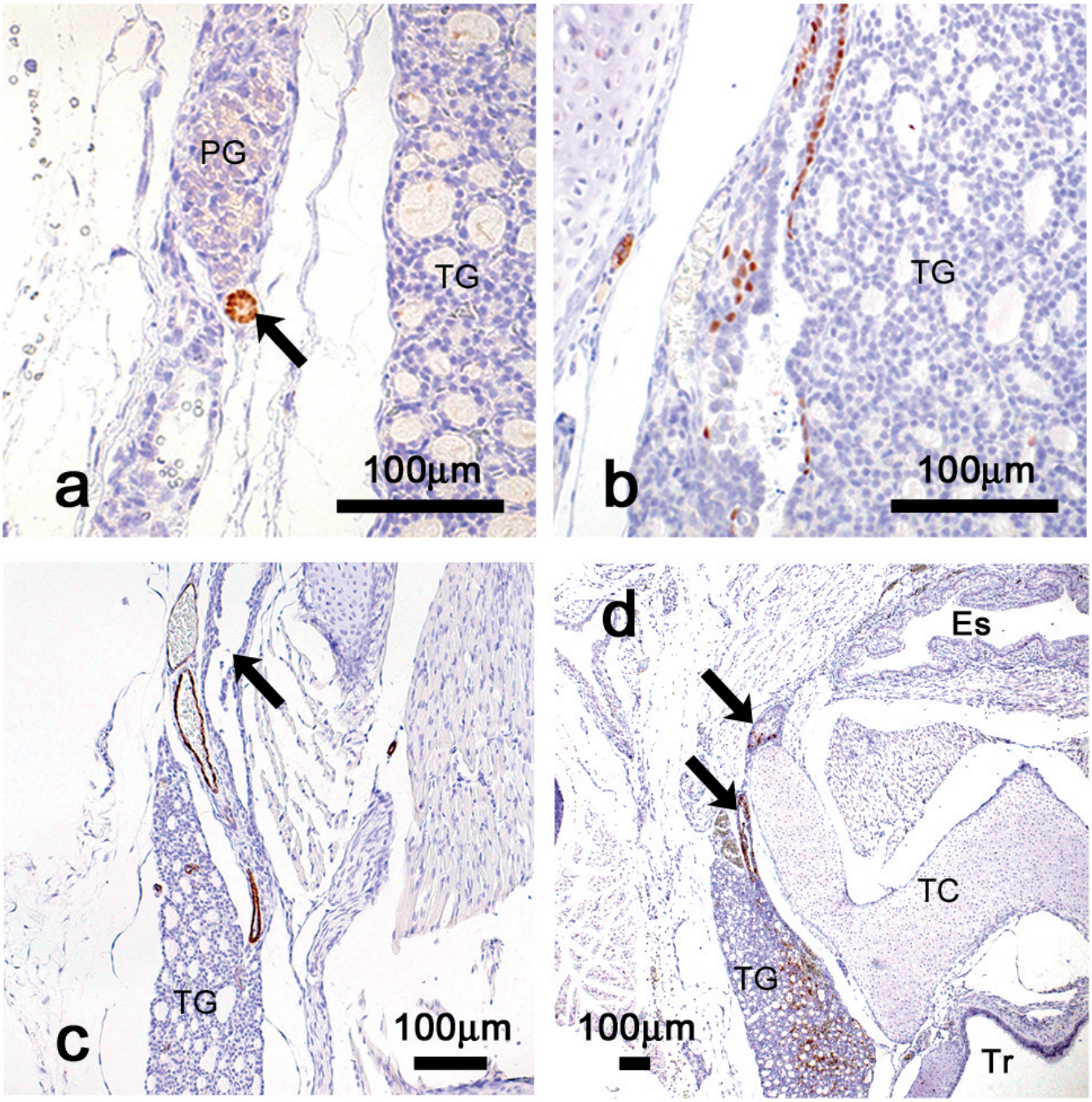

Fig. 3. Histological features around the laryngeal pharynx in neonatal HIS/Hiph at postnatal day 1. **a.** Immunohistochemistry of p63 in parathyroid gland. Arrow indicates narrow lumen of p63-positive cells. **b.** Immunohistochemistry of p63 in fossula extended from piriform fossa. **c.** Immunohistochemistry of α-smooth muscle actin around the thyroid gland. Arrow indicates the fossula extended from piriform fossa. **d.** Immunohistochemistry of calcitonin in fossula extended from piriform fossa. Arrow indicates ductal structure containing calcitonin-positive C-cells. Es: esophagus, PG: parathyroid gland, TC: thyroid cartilage, TG: thyroid gland, Tr: trachea.

2g). Interestingly, calcitonin-positive cells were found to be sparsely distributed in the epithelium of the ductal structures (Fig. 2i) and were densely distributed around the ends of the thyroid glands in HIS/Hiph (Fig. 2j). Lumen of the ductal structures contained numerous cell debris and neutrophils, but not thyroglobulin (Fig. 2d-f,k).

Next, we examined the HIS/Hiph at postnatal day 1 for the appearance of cystic and ductal structures in the neonatal period. The p63-positive cells were found in the parathyroid glands, and they formed narrow lumens at their caudal end (Fig. 3a). Ductal structures containing p63-positive cells were also observed in the lobes of the thyroid glands (Fig. 3b), which ran along the α-SMA positive superior thyroid artery (Fig. 3c). Calcitonin-positive cells resided exclusively within the thyroid gland and the ductal structures, but were not found in the surrounding connective tissues, the esophagus and the trachea (Fig. 3d). Thus, we found that the cystic and the ductal structures were already present at the neonatal stage.

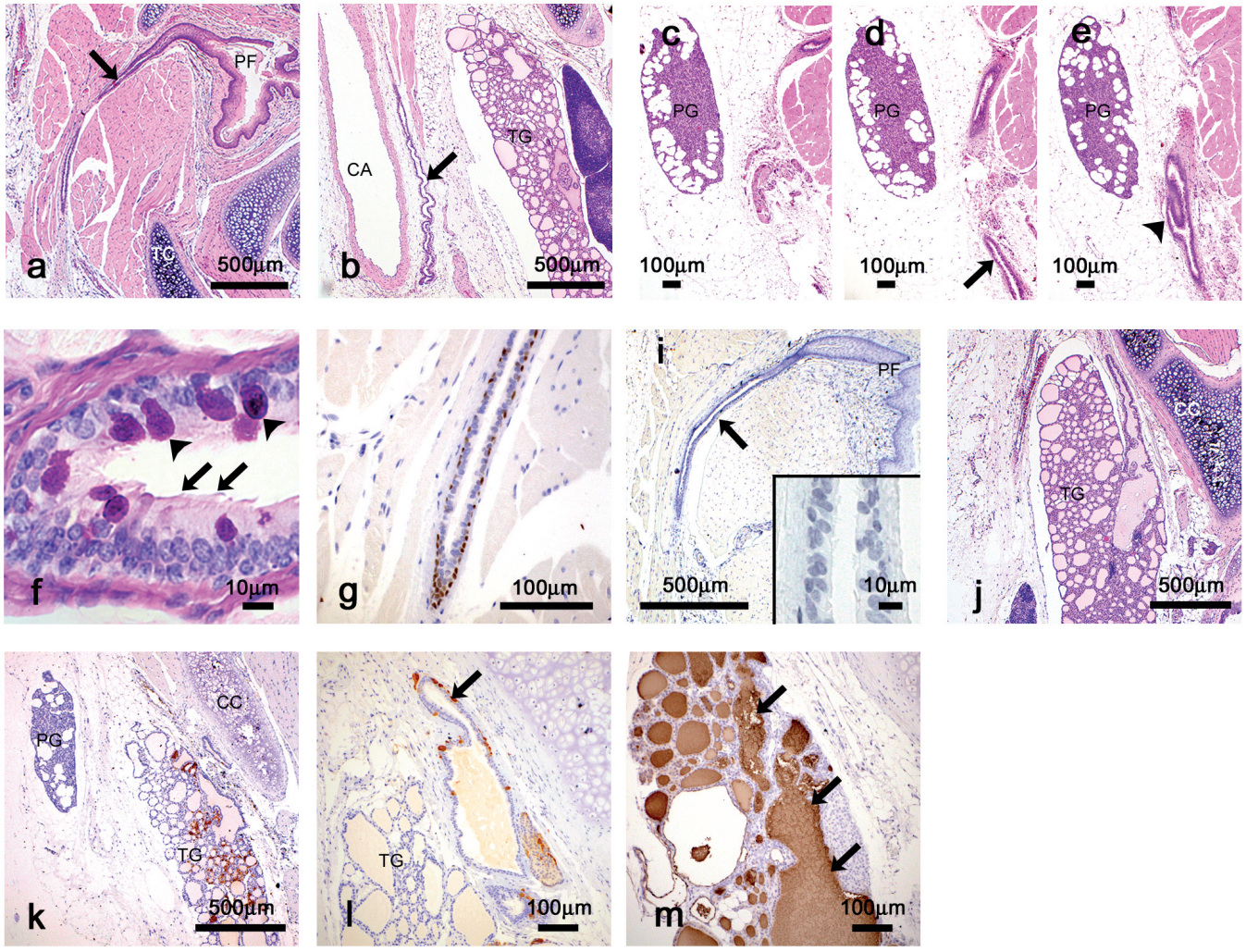

Fig. 4. Ductal structures extending from piriform fossa in HIS/Mz cotton rats. **a, b.** Horizontal sections of the laryngeal pharynx. These sections were prepared at 50 μm intervals. Arrows indicate the ductal structures. HE staining. **c-e.** Horizontal sections of the ductal structures extended from piriform fossa at 50 μm intervals. HE staining. Arrow and arrowhead indicate the branches descending caudally and toward parathyroid gland, respectively. HE staining. **f.** Epithelial structure of the ductal structures. PAS staining. Arrows and arrowheads indicate ciliated epithelial cells and goblet cells, respectively. **g.** Immunohistochemistry of p63 in the ductal structures. **i.** Immunohistochemistry of calcitonin in the ductal structure. Arrow indicates the fossula extended from piriform fossa. The inset shows a higher magnification of the epithelium of the ductal structures. **j.** Horizontal section of the thyroid gland in HIS/Mz. HE staining. **k.** Immunohistochemistry of calcitonin in the thyroid gland. It is noted that the calcitonin-positive cells are not present in the parathyroid glands. **l.** Immunohistochemistry of calcitonin in ductal structure of the thyroid gland. Arrow indicates the ductal structure extending from thyroid gland. **m.** Immunohistochemistry of thyroglobulin in cystic structure of the thyroid gland. Arrows indicate the cystic structure. CA: common carotid artery, CC: cricoid cartilage, PF: piriform fossa, PG: parathyroid gland, TC: thyroid cartilage, TG: thyroid gland.

Ductal structures extended from the piriform fossa in HIS/Mz cotton rats

In HIS/Mz, the fossulae at the piriform fossa continued as ductal structures, running downward, along the outer side of the thyroid glands, parallel to the common carotid artery (Fig. 4a,b). The opening sites of the fossulae at piriform fossa were slightly more cranial in HIS/Mz than in HIS/Hiph (Figs. 2a, 4a). In one of the five cases where ductal structures were observed, the ductal structures branched near the parathyroid glands (Fig. 4c-e); one branch descended caudally (Fig. 4d), and another one ran toward the parathyroid glands (Fig. 4e). In all the five cases, the ductal structures ended at the connective tissues around the parathyroid glands, but were not connected to the parathyroid glands. Similar to the cystic structures found in the intrathoracic thymus and the parathyroid glands, the lining of the ductal structures was composed of columnar ciliated epithelium along with a few goblet cells (Fig. 4f). Although the basal cells showed p63-positive reactions, calcitonin-positive cells did not appear in the epithelium of the ductal structures (Fig. 4g,i).

In addition to the ductal structures extended from piriform fossa, cystic structures appeared in the same site of the thyroid glands as in HIS/Hiph (Fig. 4j). Although the ductal structures extended from the thyroid glands, the structures did not connect to the piriform fossa in contrast to HIS/Hiph (Figs. 2a, 4j). These structures were observed bilaterally in all animals of both sexes. Calcitonin-positive C-cells were observed around the cystic structure and within the epithelium of their ductal structures (Fig. 4k,l). Amorphous content was observed in the cystic structures, and was positive for thyroglobulin (Fig. 4m).

Discussion

Cotton rats possess pharyngeal pouch remnants

The morphological features of the laryngeal pharynx and pharyngeal pouch-derived organs differed between cotton rats and other rodents. Briefly, both the cotton rat strains frequently possessed thymic tissues in the cervix. In mice and rats, the cervical thymuses are recognized as ectopic and are formed during the migration of fetal thymus (Pearse, 2006). Further, in cotton rats, the cystic structures appeared in the intrathoracic thymus and the parathyroid glands, and the basal cells of their epithelium were positive for p63 protein, a marker for pharyngeal pouch remnants (Kameda et al., 2009; Ríos Moreno et al., 2011). Similar cystic structures were reported in other animal species such as "thymopharyngeal duct cysts" and "parathyroid cysts," respectively, and were documented as remnants originating from the pharyngeal pouches (Kameda, 1971, 1987; Capen and Rosol 1989; Pearse, 2006). In addition, the cystic structures were already present in the parathyroid glands of the neonatal HIS/Hiph. Therefore, we demonstrated that cotton rats frequently possessed remnants originating from pharyngeal pouches in the thymus and the parathyroid glands.

The fossulae at the piriform fossa were found in all HIS/Hiph animals including neonates, and about half the HIS/Mz animals. Similar fossulae have been reported in humans, where they appear due to congenital anomalies derived from third and fourth pharyngeal pouches known as the "third/fourth branchial pouch sinuses" or

Table 3. Site of presentation of fossulae from piriform fossa.

	HIS/Hiph			HIS/Mz		
	Total	Male	Female	Total	Male	Female
Number of cases	36	18	18	5	3	2
Left	12 (33.3%)	9 (50.0%)	3 (16.7%)	5 (100%)	3 (100%)	2 (100%)
Right	6 (16.7%)	3 (16.7%)	3 (16.7%)	0 (0%)	0 (0%)	0 (0%)
Bilateral	18 (50.0%)	6 (33.3%)	12 (66.6%)	0 (0%)	0 (0%)	0 (0%)

Table 4. Histological features of piriform sinus fistula in cotton rats.

	HIS/Hiph	HIS/Mz
Site of opening	Apex of piriform fossa	Apex of piriform fossa, but slightly more cranial than HIS/Hiph
Route	Medial side of the thyroid glands	Outer side of the thyroid glands
Site of ending	Internal side of the upper pole of the thyroid glands	Connective tissues around the parathyroid glands
Terminal structure	No-dilations, dilations, and branches	No-dilation
Epithelium	Stratified squamous and cuboidal epithelium	Columnar ciliated epithelium and some goblet cells
p63 expression	Positive	Positive
C-cells	Present	Absent
Inflammation	Neutrophil infiltration and cell debris	No cellular inflammation

"piriform sinus fistula (PSF)", according to their embryological origin or morphological features, respectively (Rea et al., 2004; Nicoucar et al., 2009, 2010). These terms are still controversial in humans; for the former term, the embryological origins of these anomalies are not fully known, and the latter term was considered incorrect because most cases of the congenital third and fourth pouch anomalies are not congenital fistula (Rea et al., 2004). In humans, the PSF are lined with squamous stratified epithelium (58-76%) and ciliated epithelium (11-35%). In cotton rats, although the embryological origin of the pharyngeal pouch derivatives has not been directly demonstrated yet, the morphological and histological characteristics of the fossulae of the piriform fossa were similar to those in humans. Therefore, we considered that "PSF" was the most appropriate homologous term for referring to the ductal structures originating from the piriform fossa in cotton rats.

Origin of the PSF in cotton rats

The morphological and histological features of the PSF differed between the two inbred cotton rat strains (Fig. 5, Table 4). First, although the PSF opened near the apex of the piriform fossa in both HIS/Hiph and HIS/Mz, it opened slightly more cranially in the latter. Second, the PSF passed the medial side of the thyroid glands and ended within the thyroid glands in HIS/Hiph, whereas it passed and ended outside the thyroid glands in HIS/Mz. Third, the lining of the PSF was primarily stratified squamous and cuboidal epithelium in HIS/Hiph, whereas it was columnar ciliated epithelium with a few goblet cells in HIS/Mz. Lumen of the PSF contained numerous neutrophils and cell debris only in HIS/Hiph. These results suggested that the PSF originated from different primordia between the two strains. The PSF in HIS/Hiph terminated with branched structures, and the branching increased with age. In the branched end of the PSF in HIS/Hiph, proliferating epithelial cells were frequently observed, and their lumens typically contained large amounts of cell debris and numerous neutrophils. Taken together, our observations indicate that age-related changes at the end of PSF might be caused by hyperplasia of the epithelium in response to inflammation.

In HIS/Hiph, the calcitonin-positive C-cells, derivatives of the ultimobranchial body, were present in the epithelium of the PSF, and the epithelial structures were consistent with that of ultimobranchial body cysts in rats (Vázquez-Román et al., 2013). The basal cells of the PSF expressed p63, which is used as a marker for ultimobranchial body remnants (Kusakabe et al., 2006; Ozaki et al., 2011). More importantly, in cotton rats, parathyroid glands were not included within the thyroid glands unlike in other rodents (Grevellec and Tucker, 2010). These results indicated that the PSF in HIS/Hiph were remnants of the ultimobranchial body. In HIS/Mz, cystic structures also appeared in the thyroid glands. The lining epithelium of the cystic structures contained C-cells, indicating that the cystic structures were also the ultimobranchial body remnants.

In HIS/Mz, the PSF ended near the parathyroid glands, and in one case, the PSF branched caudally, in the direction of the thymus. During mammalian fetal development, the thymus and parathyroid gland III (derived from third pouches) migrate caudally, forming the thymopharyngeal duct (Grevellec and Tucker, 2010). The epithelial structures of the PSF in HIS/Mz were consistent with the cystic structures found in thymus and parathyroid glands. Furthermore, C-cells in some mammals occur in parathyroid gland IV but not in parathyroid gland III (Kameda, 1971). In HIS/Mz, C-cells did not appear in the parathyroid glands. Taken together, these results indicate that the PSF in HIS/Mz were remnants of the thymopharyngeal duct. In future, the clarification of the developmental stages of the pharyngeal pouches in cotton rats would help us to

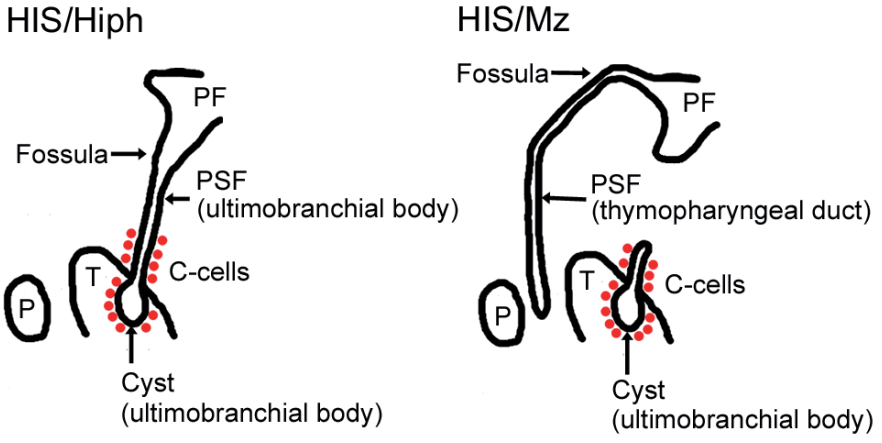

Fig. 5. Route and the embryological origin of piriform sinus fistula in cotton rats. PSF: piriform sinus fistula, P: parathyroid gland, PF: piriform fossa, T: thyroid gland. Red dots represent C-cells.

elucidate the developmental origin of PSF.

Our results also suggest that genetic factors might affect the development of the PSF. Although several genes related to the morphogenesis of pharyngeal pouch-derived organs have been discovered in zebrafish and mice (Fagman and Nilsson, 2010), those related to PSF have not been reported. In mice, NKX2-1 plays an important role in the formation of ultimobranchial body cysts, in addition to the survival of ultimobranchial body cells and the dissemination of the ultimobranchial body into the thyroid diverticulum (Kusakabe et al., 2006; Ozaki et al., 2011). Although, like cotton rats, NKX2-1 heterozygous mice form ultimobranchial body cysts on the dorsal side of the thyroid glands, the occurrence of the PSF has not been confirmed (Kusakabe et al., 2006). Our results might indicate that formation of the PSF is controlled by novel genes or polygenic factors. In addition, differentiation of presumed ultimobranchial body into thyroid follicle which produced thyroglobulin was strain-dependent in the cotton rats. In human, ultimobranchial body remnants form the typical thyroid follicular epithelium which may produce thyroglobulin, or the stratified squamous epithelium which is negative for thyroglobulin (Williams et al., 1989; Ríos Moreno et al., 2011). Further genetic studies such as whole-genome sequencing are needed to elucidate the detailed mechanisms of these strain differences, as the genetic information available on cotton rats is scarce.

Cotton rats as animal models for human PSF

In humans, the PSFs are relatively rare congenital malformations, representing up to 10% of all pharyngeal pouch anomalies (Goff et al., 2012). The human PSF occurs primarily left-sided (89-94%), and presents itself with either neck abscess (39-42%) or acute suppurative thyroiditis (33-46%) (Nicoucar et al., 2009, 2010). In the present study, the PSFs mainly occurred also on the left side in HIS/Mz but bilaterally in HIS/Hiph. These differences in the laterality between HIS/Hiph and humans might be affected by the incidence of the PSF, which is 100% in HIS/Hiph. Similar to the human PSFs that sometimes form branches in the thyroid glands (Miyauchi et al., 1992; Nicoucar et al., 2009, 2010), PSF of HIS/Hiph also ended in branched structures, and the branching increased with age. In HIS/Hiph, proliferating cells were frequently observed in the epithelium of the branched end of PSF, suggesting that the epithelial proliferation might affect the morphology of the terminal structures in PSFs. These similarities of PSFs between human and cotton rat suggest that the cotton rat might be a useful animal model for studying human PSF.

In humans, the diagnostic markers for estimating the origin of PSF are still not established. Although the theoretical route of the human PSF originating from third and fourth pharyngeal pouches has been proposed, PSFs do not follow the proposed route in many cases (James et al., 2007; Thomas et al., 2010). The theory of ultimobranchial body origin has also been proposed based on the histological distribution of C-cells; however, their routes have not been demonstrated yet (Miyauchi et al., 1992; Himi and Kataura, 1995; Seki and Himi, 2007). Interestingly, the route of the PSF in HIS/Hiph was consistent with the one observed in humans (James et al., 2007). These results suggest that the route of the PSFs observed in cotton rats might serve as a useful diagnostic marker for their origin.

In conclusion, cotton rats frequently possessed several pharyngeal pouch remnants including the PSF. This rodent might serve as a novel animal model to elucidate the developing mechanisms of pharyngeal pouch derivatives and PSF.

Acknowledgements. We would like to acknowledge Daisuke Nakamura, Saori Nakamura, Shinobu Sato, Keisuke Yokoyama of Sankyo Labo Service Corporation, INC., and Junko Horii, Tomoko Tashiro of University of Miyazaki for their assistance of the animal care. This work was partially supported by JSPS KAKENHI Grant Numbers 14F04400 and 26450439.

References

Capen C.C. and Rosol T.J. (1989). Recent advances in the structure and function of the parathyroid gland in animals and the effects of xenobiotics. Toxicol. Pathol. 17, 333-345.

Fagman H. and Nilsson M. (2010). Morphogenesis of the thyroid gland. Mol. Cell. Endocrinol. 323, 35-54.

Faith R.E., Montgomery C.A., Durfee W.J., Aguilar-Cordova E. and Wyde P.R. (1997). The cotton rat in biomedical research. Lab. Anim. Sci. 47, 337-345.

Goff C.J., Allred C. and Glade R.S. (2012). Current management of congenital branchial cleft cysts, sinuses, and fistulae. Curr. Opin. Otolaryngol. Head Neck Surg. 20,533-539.

Grevellec A. and Tucker A.S. (2010). The pharyngeal pouches and clefts: Development, evolution, structure and derivatives. Semin. Cell Dev. Biol. 21, 325-332.

Himi T. and Kataura A. (1995). Distribution of C cells in the thyroid gland with pyriform sinus fistula. Otolaryngol. Head Neck Surg. 112, 268-273.

Ichii O., Nakamura T., Irie T., Kouguchi H., Nakamura D., Nakamura S., Sato S., Yokoyama K., Horino T., Sunden Y., Elewa Y.H. and Kon Y. (2016). Female cotton rats (*Sigmodon hispidus*) develop chronic anemia with renal inflammation and cystic changes. Histochem. Cell Biol. 146, 351-362.

James A., Stewart C., Warrick P., Tzifa C. and Forte V. (2007). Branchial sinus of the piriform fossa: reappraisal of third and fourth branchial anomalies. Laryngoscope 117, 1920-1924.

Johansson E., Andersson L., Örnros J., Carlsson T., Ingeson-Carlsson C., Liang S., Dahlberg J., Jansson S., Parrillo L., Zoppoli P., Barila G.O., Altschuler D.L., Padula D., Lickert H., Fagman H. and Nilsson M. (2015). Revising the embryonic origin of thyroid C cells in mice and humans. Development 142, 3519-3528.

Kameda Y. (1971). The occurrence and distribution of the parafollicular cells in the thyroid, parathyroid IV and thymus IV in some mammals. Arch. Histol. Jpn. 33, 283-299.

Kameda Y. (1987). Immunohistochemical demonstration of keratins in the cysts of thyroid glands, parathyroid glands, and C-cell

complexes of the dog. Am. J. Anat. 18, 87-99.

Kameda Y., Ito M., Nishimaki T. and Gotoh N. (2009). FRS2α is required for the separation, migration, and survival of pharyngeal-endoderm derived organs including thyroid, ultimobranchial body, parathyroid, and thymus. Dev. Dyn. 238, 503-513.

Kusakabe T., Hoshi N. and Kimura S. (2006). Origin of the ultimobranchial body cyst: T/ebp/Nkx2.1 expression is required for development and fusion of the ultimobranchial body to the thyroid. Dev. Dyn. 235, 1300-1309.

Miyauchi A., Matsuzuka F., Kuma K. and Katayama S. (1992). Piriform sinus fistula and the ultimobranchial body. Histopathology 20, 221-227.

Nicoucar K., Giger R., Pope H.G. Jr., Jaecklin T. and Dulguerov P. (2009). Management of congenital fourth branchial arch anomalies: a review and analysis of published cases. J. Pediatr. Surg. 44, 1432-1439.

Nicoucar K., Giger R., Jaecklin T., Pope H.G. Jr. and Dulguerov P. (2010). Management of congenital third branchial arch anomalies: a systematic review. Otolaryngol. Head Neck Surg. 142, 21-28.

Niewiesk S. and Prince G. (2002). Diversifying animal models: the use of hispid cotton rats (*Sigmodon hispidus*) in infectious diseases. Lab. Anim. 36, 357-372.

Ozaki T., Nagashima K., Kusakabe T., Kakudo K. and Kimura S. (2011). Development of thyroid gland and ultimobranchial body cyst is independent of p63. Lab. Invest. 91, 138-146.

Rea P.A., Hartley B.E. and Bailey C.M. (2004). Third and fourth branchial pouch anomalies. J. Laryngol. Otol. 118, 19-24.

Ríos Moreno M.J., Galera-Ruiz H., De Miguel M., López M.I., Illanes M. and Galera-Davidson H. (2011). Immunohistochemical profile of solid cell nest of thyroid gland. Endocr. Pathol. 22, 35-39.

Seki N. and Himi T. (2007). Retrospective review of 13 cases of pyriform sinus fistula. Am. J. Otolaryngol. 28, 55-58.

Setoguchi Y., Danel C. and Crystal R.G. (1994). Stimulation of erythropoiesis by in vivo gene therapy: physiologic consequences of transfer of the human erythropoietin gene to experimental animals using an adenovirus vector. Blood 84, 2946-2953.

Shrime M., Kacker A., Bent J. and Ward R.F. (2003). Fourth branchial complex anomalies: a case series. Int. J. Pediatr. Otorhinolaryngol. 67, 1227-1233.

Thomas B., Shroff M., Forte V., Blaser S. and James A. (2010). Revisiting imaging features and the embryologic basis of third and fourth branchial anomalies. Am. J. Neuroradiol. 31, 755-760.

Vázquez-Román V., Utrilla J.C., Fernández-Santos J.M., Conde E., Bernabé R., Sampedro C. and Martín-Lacave I. (2013). Postnatal fate of the ultimobranchial remnants in the rat thyroid gland. J. Morphol. 274, 725-732.

Waldum H.L., Rørvik H., Falkmer S. and Kawase S. (1999). Neuroendocrine (ECL cell) differentiation of spontaneous gastric carcinomas of cotton rats (*Sigmodon hispidus*). Lab. Anim. Sci. 49, 241-247.

Accepted November 21, 2017